Nonuniform TFA for periodic masonry walls

Sonia Marfia, Elio Sacco
Università di Cassino, Dipartimento di Meccanica, Strutture, Ambiente e Territorio, via G. di Biasio 43, 03043 Cassino (Italy)
marfia@unicas.it; sacco@unicas.it

ABSTRACT. In the present paper, the TFA homogenization procedure is extended to the case of nonuniform eigenstrain in the inclusions, in order to deduce the overall response of regular masonry arrangements to be used for the multiscale analysis of masonry walls. Special constitutive laws, based on damage and plasticity models, are adopted for the mortar. Nonlinear behavior is considered even for some subsets of the blocks; in fact, nonlinear damage and plasticity effects are introduced in the subsets of the block aligned with the head mortar joints. Numerical examples of homogenization are carried out, comparing the nonlinear mechanical response of the masonry obtained performing the proposed homogenization technique with the results recovered by evolutive nonlinear finite element analyses.

KEYWORDS. Periodic Masonry; Multiscale Analysis; Damage-Friction; Finite Element Analysis.

INTRODUCTION

The masonry is a composite material obtained assembling blocks of different nature and shape connected by mortar beds. The global mechanical response of the composite material can be obtained adopting homogenization procedures, that study a representative volume element (RVE) determining the behavior of the homogenized equivalent material. In order to develop a structural study, in which the nonlinear response of the masonry material is derived from a micromechanical analysis, a micro-macro approach, in other words a multiscale approach, has to be performed. The multiscale technique consists in the structural modeling through two different scales: one scale at the continuum mechanics structural level, macro-scale, and one scale at the material level, micro-scale, able to distinguish the single heterogeneities that are present in the masonry material. The development and the use of multiscale procedures is a complex task as it is necessary to solve the micromechanical problem and to adopt the obtained results in order to perform the structural analysis.

It can be remarked that the masonry can be characterized by different arrangements of the blocks that can be positioned in regular or irregular arrays. In the case of composite material with periodic microstructure, it is possible to consider a unit repetitive cell (UC) in order to study the constitutive behavior of the composite [1, 2].

Simplified micromechanical approaches, derived for the particular microstructural geometry of masonry material, have been developed, among the others, in References [3-6].

A multiscale procedure was presented by Luciano and Sacco [7], assuming that fractures can develop only in the mortar material. For the periodic unit cell, all the possible states, characterized by different arrangements of cracks in mortar, are identified. Then, crack growth and evolutive relations are provided.

Indeed, a major problem in the multiscale analysis is the development of an effective, i.e. simple and accurate, homogenization procedure. It could be emphasized that, for the masonry material, the homogenization is not a simple task as, even if regular periodic masonry is considered, the geometry of the UC is still complex.

The Transformation Field Analysis (TFA) is an interesting approach for solving the nonlinear micro-mechanical homogenization problem. It was initially proposed by Dvorak [8] and, then, applied to plasticity and visco-plasticity problems by Fish and Shek [9]. According to TFA approach, the inelastic strain, is assumed to be uniform in each individual phase of the composite. Chaboche et al. [10] improved the TFA for deriving the nonlinear behavior of

damaging composites, subdividing each phase into sub-domains, at the expense of increasing the complexity of the model. Michel and Suquet [11] presented a nonuniform TFA procedure for determining the overall behavior of nonlinear composite materials. The use of the TFA requires the computation of localization and transformation tensors. When the geometry of the microstructure is complex, as in the case of masonry material, numerical techniques can be adopted. In fact, the finite element method or the fast Fourier transform technique are able to accurately evaluate local stress and strain fields, so that the correct nonlinear behavior of the phases can be described.
Recently, Sacco [12] and Addessi et al. [13] presented a nonlinear homogenization procedure for the Cauchy and Cosserat masonry models based on TFA, making use of the superposition of the effects and of the finite element method.
In the present paper, the TFA homogenization procedure is extended to the case of nonuniform eigenstrain in the inclusions, in order to deduce the overall response of regular masonry arrangements to be used for the multiscale analysis of masonry walls.
Each phase of the unit cell, i.e. mortar and bricks, is decomposed in subsets. Special constitutive laws, based on damage and plasticity models, are adopted for the mortar. Nonlinear behavior is considered even for some subsets of the blocks; in fact, nonlinear damage and plasticity effects are introduced in the subsets of the block aligned with the head mortar joints.
The TFA is extended to the nontrivial case of bilinear distribution of the eigenstrain in the subsets. The nonlinear governing equations are deduced and a numerical procedure is proposed. Numerical examples of homogenization are carried out, comparing the nonlinear mechanical response of the masonry obtained performing the proposed homogenization technique with the results recovered by evolutive nonlinear finite element analyses. The numerical results demonstrate that the proposed enhancement of the classical TFA leads to very satisfactory results.

NONLINEAR HOMOGENIZATION FOR PERIODIC MASONRY

The masonry is considered as a composite, i.e. heterogeneous, material composed by bricks and mortar organized in a very regular geometry at the microscale level. In fact, the bricks are connected by horizontal and vertical joints of mortar, generating a periodic microstructure. Hence, the regular masonry material is a periodic composite material. A special, but very common, masonry texture is studied in the following. The considered Unit Cell (UC) completely defining the masonry material arrangement is illustrated in Fig. 1. The chosen UC is characterized by a rectangular shape with dimensions $2a_1$ and $2a_2$, parallel to the coordinate axes x_1 and x_2, as shown in Fig. 1. It accounts for all the geometric and constitutive information of the masonry components; the mortar thickness is denoted by s and the brick sizes by b and h.

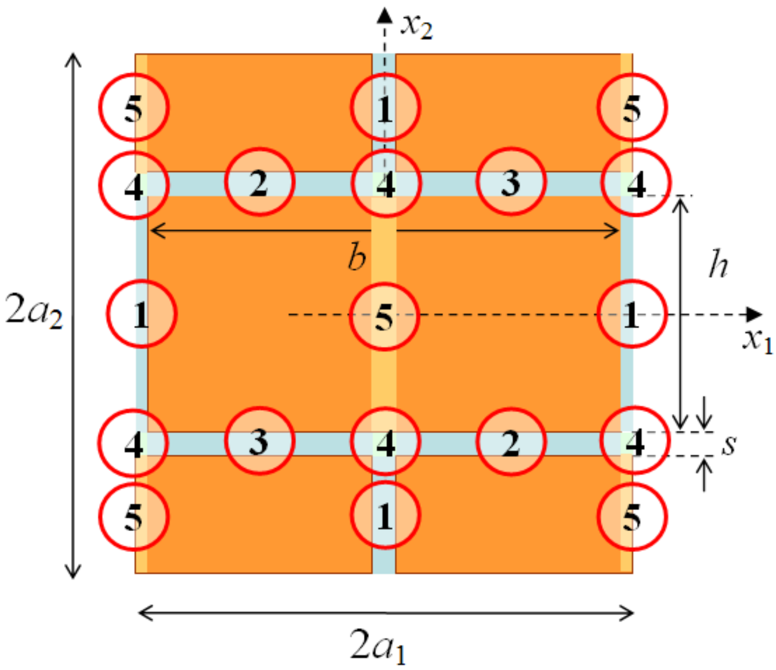

Figure 1: Unit cell for repetitive masonry.

It can be remarked that the whole UC is divided in subsets, some of which are indicated by a number form 1 to 5. In particular, subset 1 indicates the mortar head joints, subset 2 and 3 the bed joints, 4 the head-bed mortar intersection and 5 is the vertical part of the bricks aligned with the mortar head joints. Indeed, it is assumed that the numbered subsets are responsible for the nonlinear behavior of the masonry.

Mortar

A very special constitutive law, based on the mechanical model proposed by Sacco [12], is considered for the mortar. The constitutive law accounts for the coupling of the damage and friction phenomena occurring in the mortar joints during the strain history [6].

A local coordinate system is introduced: *H* denotes the horizontal axis and *V* is the vertical direction, as reported in Fig. 2.

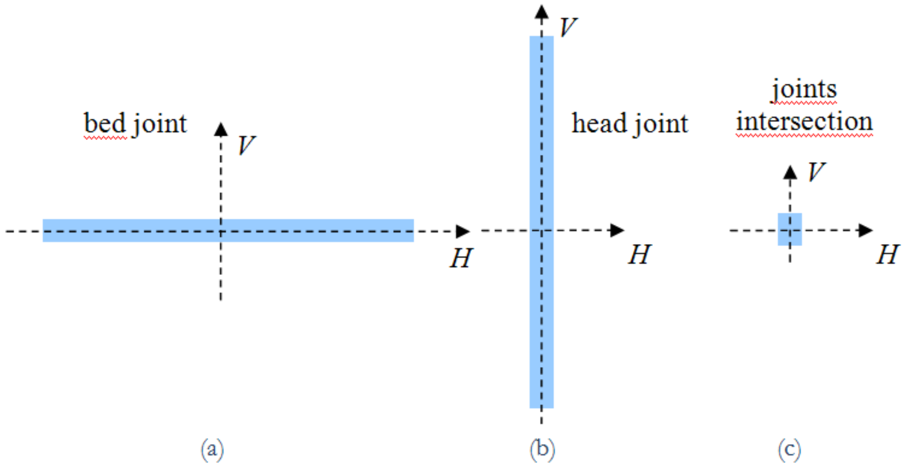

Figure 2: Coordinate system for (a) bed and (b) head joints.

The Representative Mortar Element RME, defining the constitutive behavior at a typical point of the mortar, is introduced. A micromechanical analysis of the RME allows to define the damage variable D as the ratio between the damaged and the total representative area.

Denoting with the superscripts ^{u} and ^{d} the quantities referred to the undamaged and damaged part of the RME, respectively, and adopting the Voigt notation, the stress vector $\boldsymbol{\sigma}^M = \left\{ \sigma_H^M \quad \sigma_V^M \quad \tau^M \right\}^T$ is obtained by the relationship:

$$\boldsymbol{\sigma}^M = (1-D)\boldsymbol{\sigma}^u + D\boldsymbol{\sigma}^d \tag{1}$$

where:

$$\boldsymbol{\sigma}^u = \mathbf{C}^M \boldsymbol{\varepsilon}^M \qquad \boldsymbol{\sigma}^d = \mathbf{C}^M \left(\boldsymbol{\varepsilon}^M - \mathbf{c} - \boldsymbol{\varepsilon}^p \right) \qquad \text{with } \mathbf{C}^M = \begin{bmatrix} C_{HH}^M & C_{HV}^M & 0 \\ C_{VH}^M & C_{VV}^M & 0 \\ 0 & 0 & G^M \end{bmatrix} \tag{2}$$

being $\boldsymbol{\varepsilon}^M = \left\{ \varepsilon_H^M \quad \varepsilon_V^M \quad \gamma^M \right\}^T$ the strain vector and $\mathbf{C}^M$ the elasticity matrix of the mortar. The inelastic strain vectors $\mathbf{c}$ and $\boldsymbol{\varepsilon}^p$ are defined in the damaged part of the RME and account for the unilateral effect and the possible friction sliding, respectively. In particular, it is assumed:

$$\mathbf{c} = \left\{ \tilde{h}\,\varepsilon_H \quad \tilde{h}\,\varepsilon_V \quad \tilde{h}\,\gamma \right\}^T \tag{3}$$

Where $\tilde{h} = \max\left\{ h(\varepsilon_H), h(\varepsilon_V) \right\}$; $h(\varepsilon_\bullet)$ is the Heaviside function, which assumes the following values: $h(\varepsilon_\bullet) = 0$ if $\varepsilon_\bullet \le 0$ and $h(\varepsilon_\bullet) = 1$ if $\varepsilon_\bullet > 0$, where $\bullet$ stands for H or V . In such a way, setting $\boldsymbol{\varepsilon}^p = \mathbf{0}$, the following cases can occur:

$$\begin{array}{llll} \varepsilon_H > 0 \quad \varepsilon_V > 0 & \mathbf{c} = \left\{ \varepsilon_H \quad \varepsilon_V \quad \gamma \right\}^T & \boldsymbol{\varepsilon} - \mathbf{c} = \left\{ 0 \quad 0 \quad 0 \right\}^T & \boldsymbol{\sigma}^d = \left\{ 0 \quad 0 \quad 0 \right\}^T \\ \varepsilon_H > 0 \quad \varepsilon_V \leq 0 & \mathbf{c} = \left\{ \varepsilon_H \quad \varepsilon_V \quad \gamma \right\}^T & \boldsymbol{\varepsilon} - \mathbf{c} = \left\{ 0 \quad 0 \quad 0 \right\}^T & \boldsymbol{\sigma}^d = \left\{ 0 \quad 0 \quad 0 \right\}^T \\ \varepsilon_H \leq 0 \quad \varepsilon_V > 0 & \mathbf{c} = \left\{ \varepsilon_H \quad \varepsilon_V \quad \gamma \right\}^T & \boldsymbol{\varepsilon} - \mathbf{c} = \left\{ 0 \quad 0 \quad 0 \right\}^T & \boldsymbol{\sigma}^d = \left\{ 0 \quad 0 \quad 0 \right\}^T \\ \varepsilon_H \leq 0 \quad \varepsilon_V \leq 0 & \mathbf{c} = \left\{ 0 \quad 0 \quad 0 \right\}^T & \boldsymbol{\varepsilon} - \mathbf{c} = \left\{ \varepsilon_H \quad \varepsilon_V \quad \gamma \right\}^T & \boldsymbol{\sigma}^d = \left\{ \sigma_H^d \quad \sigma_V^d \quad \tau^d \right\}^T \end{array} \tag{4}$$

The inelastic strain $\boldsymbol{\varepsilon}^p$ is characterized by the first two components equal to zero, and by the third component accounting for the sliding: $\boldsymbol{\varepsilon}^p = \left\{ 0 \quad 0 \quad \gamma^p \right\}$. The evolution of the inelastic slip strain component γ^p is governed by the classical Coulomb yield functions:

$$\begin{array}{l} \varphi_H\left(\boldsymbol{\sigma}^d\right) = \mu \, {\sigma_H}^d + \left|\tau^d\right| \\ \varphi_V\left(\boldsymbol{\sigma}^d\right) = \mu \, {\sigma_V}^d + \left|\tau^d\right| \end{array} \tag{5}$$

where μ is the friction parameter. The non-associated flow rule is considered:

$$\dot{\gamma}^p = \dot{\lambda} \frac{\tau^d}{\left|\tau^d\right|} \qquad \text{with} \qquad \begin{array}{c} \dot{\lambda} \geq 0 \quad \varphi\left(\boldsymbol{\sigma}^d\right) \leq 0 \\ \dot{\lambda} \, \varphi\left(\boldsymbol{\sigma}^d\right) = 0 \end{array} \tag{6}$$

About the evolution of the damage parameter *D*, a model which accounts for the coupling of mode I and mode II of fracture is considered. The three quantities η_H, η_V and η_γ, which depend on first cracking strains $\varepsilon_{H,o}$, $\varepsilon_{V,o}$ and γ_o, on the peak value of the stresses $\sigma_{H,o}$, $\sigma_{V,o}$ and τ_o and on the fracture energies G_{HcI}, G_{VcI} and G_{cII}, respectively, are introduced:

$$\eta_H = \frac{\varepsilon_{H,o} \, \sigma_{H,o}}{2 \, G_{HcI}} \qquad \eta_V = \frac{\varepsilon_{V,o} \, \sigma_{V,o}}{2 \, G_{VcI}} \qquad \eta_\gamma = \frac{\gamma_o \, \tau_o}{2 \, G_{cII}} \tag{7}$$

Then, the strain ratios are determined as:

$$\eta = 1 - \frac{1}{\alpha^2} \left[\left\langle \varepsilon_H^M \right\rangle^2 \eta_H + \left\langle \varepsilon_V^M \right\rangle^2 \eta_V + \left(\gamma^M \right)^2 \eta_\gamma \right] \tag{8}$$

$$\beta = \sqrt{{Y_H}^2 + {Y_V}^2 + {Y_\gamma}^2} - 1 \tag{9}$$

with

$$\alpha = \sqrt{\left\langle \varepsilon_H^M \right\rangle^2 + \left\langle \varepsilon_V^M \right\rangle^2 + \left(\gamma^M \right)^2} \quad Y_H = \frac{\left\langle \varepsilon_H^M \right\rangle}{\varepsilon_{H,o}} \quad Y_V = \frac{\left\langle \varepsilon_V^M \right\rangle}{\varepsilon_{V,o}} \quad Y_\gamma = \frac{\gamma^M}{\gamma_o} \tag{10}$$

where the bracket operator $\langle \bullet \rangle$ gives the positive part of the number $\bullet$. Finally, the damage is evaluated according to the formula:

$$D = \max_{history} \left\{ \min \left\{ 1, \frac{1}{\eta} \left(\frac{\beta}{1+\beta} \right) \right\} \right\} \tag{11}$$

In Fig. 3, the normal and shear stress-strain relationships are plotted; of course, other damage evolution laws can be used in the formulation.

Taking into account the constitutive Eqs. (2), formula (1) becomes:

$$\boldsymbol{\sigma}^M = \mathbf{C}^M \left(\boldsymbol{\varepsilon} - D \boldsymbol{\pi} \right) \tag{12}$$

where the total inelastic strain $\boldsymbol{\pi} = \mathbf{c} - \boldsymbol{\varepsilon}^p$ is introduced.

It can be remarked that the proposed mortar constitutive equations can be simplified for the bed and head joint, as schematically reported in Tab. 1.

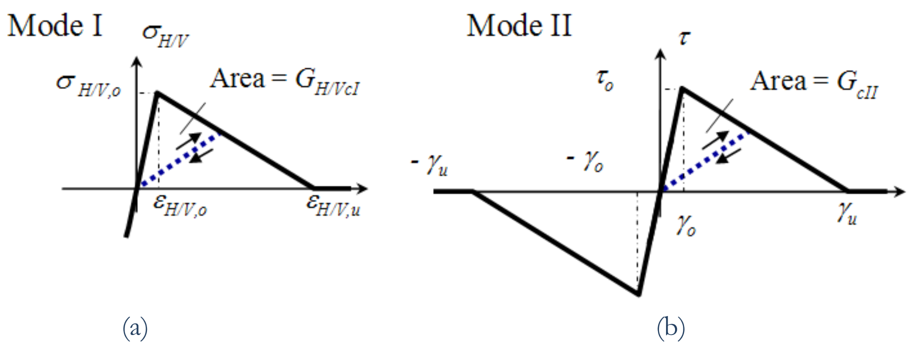

Figure 3: Stress-strain curves due to damage, (a) Mode I and (b) Mode II.

	bed joints	head joints
unilateral contact strain	$\mathbf{c}=\{h(\varepsilon_V)\varepsilon_H \;\; h(\varepsilon_V)\varepsilon_V \;\; h(\varepsilon_V)\gamma\}^T$	$\mathbf{c}=\{h(\varepsilon_H)\varepsilon_H \;\; h(\varepsilon_H)\varepsilon_V \;\; h(\varepsilon_V)\gamma\}^T$
active Coulomb yield function	$\varphi_V(\boldsymbol{\sigma}^d)=\mu\sigma_V{}^d+\lvert\tau^d\rvert$	$\varphi_H(\boldsymbol{\sigma}^d)=\mu\sigma_H{}^d+\lvert\tau^d\rvert$
damage evolution parameters	$\eta=1-\frac{1}{\alpha^2}\left[\langle\varepsilon_V^M\rangle^2\eta_V+(\gamma^M)^2\eta_\gamma\right]$ $\beta=\sqrt{\left(\frac{\langle\varepsilon_V^M\rangle}{\varepsilon_{V,o}}\right)^2+\left(\frac{\gamma^M}{\gamma_o}\right)^2}-1$ $\alpha=\sqrt{\langle\varepsilon_V^M\rangle^2+(\gamma^M)^2}$	$\eta=1-\frac{1}{\alpha^2}\left[\langle\varepsilon_H^M\rangle^2\eta_H+(\gamma^M)^2\eta_\gamma\right]$ $\beta=\sqrt{\left(\frac{\langle\varepsilon_H^M\rangle}{\varepsilon_{H,o}}\right)^2+\left(\frac{\gamma^M}{\gamma_o}\right)^2}-1$ $\alpha=\sqrt{\langle\varepsilon_H^M\rangle^2+(\gamma^M)^2}$

Table 1: Equations governing the behavior of bed and head joints.

Brick

The linear elastic constitutive law is considered for the brick. In fact, denoting by $\mathbf{C}^B$ the elastic matrix of the masonry brick, the stress-strain relationship is written in the form:

$$\boldsymbol{\sigma}^B=\mathbf{C}^B\boldsymbol{\varepsilon}^B \tag{13}$$

where $\boldsymbol{\sigma}^B=\{\sigma_1^B \;\; \sigma_2^B \;\; \tau_{12}^B\}^T$ and $\boldsymbol{\varepsilon}^B=\{\varepsilon_1^B \;\; \varepsilon_2^B \;\; \gamma_{12}^B\}^T$ are the stress and the total strain vectors in the brick, respectively.

It is assumed that the subset 5 of the brick, reported in Fig. 1, presents a nonlinear behavior; in particular, the same constitutive relationship proposed for the mortar joint is considered, assuming, of course, different values for the material parameters.

NONLINEAR HOMOGENIZATION TECHNIQUE

In the heterogeneous masonry unit cell, a set of n sub-domains Ω^i, where inelastic effects occurs, is identified. In particular, the sub-domains are introduced in the mortar joints and in a part of the brick. Denoting by $\tilde{\Omega}=\bigcup_{i=1}^{n}\Omega^i$ and by Ω the whole UC, the elastic part of the UC is denoted as Ω^e, such that $\Omega=\Omega^e\cup\tilde{\Omega}$. The UC is subjected to:

- the average strain $\overline{\mathbf{e}}$ on the whole masonry unit cell,

- the inelastic strain $\boldsymbol{\pi}^i$ in each sub-domain Ω^i $(i=1,..,n)$.

The displacement field $\mathbf{u}=\{u_1,u_2\}^T$ for periodic media is expressed by the following representation form:

$$\begin{aligned} u_1(x_1,x_2) &= \overline{\varepsilon}_1\, x_1 + \overline{\gamma}_{12}\, x_2 + \tilde{u}_1(x_1,x_2) \\ u_2(x_1,x_2) &= \overline{\gamma}_{12}\, x_1 + \overline{\varepsilon}_2\, x_2 + \tilde{u}_2(x_1,x_2) \end{aligned} \tag{14}$$

where $\mathbf{x}=(x_1,x_2)$ is the position vector of the typical point of Ω, $\overline{\boldsymbol{\varepsilon}}$ is the average strain of the cell and $\tilde{\mathbf{u}}(x_1,x_2)$ is the periodic part of the displacement [1, 2]. From formula (14), the strain vector is given by:

$$\boldsymbol{\varepsilon}(x_1,x_2) = \overline{\boldsymbol{\varepsilon}} + \tilde{\boldsymbol{\varepsilon}}\,(x_1,x_2) \tag{15}$$

where $\tilde{\boldsymbol{\varepsilon}}\,(x_1,x_2)$ is the periodic part of the strain, with null average in Ω, associated to the displacement $\tilde{\mathbf{u}}$.

The in-plane periodicity and continuity conditions lead to the following boundary conditions:

$$\begin{aligned} \tilde{\mathbf{u}}(a_1,x_2) &= \tilde{\mathbf{u}}(-a_1,x_2) \qquad \forall x_2 \in [-a_2,a_2] \\ \tilde{\mathbf{u}}(x_1,a_2) &= \tilde{\mathbf{u}}(x_1,-a_2) \qquad \forall x_1 \in [-a_1,a_1] \end{aligned} \tag{16}$$

Because of the periodicity of the solution of the micromechanical problem, it can be deduced that the parts of the unit cell denoted with the same label in Fig. 1 are characterized by the same strain and stress fields.

Average strain $\overline{\mathbf{e}}$

Let the solution of the micromechanical problem, corresponding to the prescribed value of the overall strain $\overline{\mathbf{e}}$, be determined. The strain field can be written in the following representation form:

$$\mathbf{e}(x_1,x_2) = \mathbf{R}(x_1,x_2)\,\overline{\mathbf{e}} \tag{17}$$

Where $\mathbf{R}(x_1,x_2)$ is the localization matrix, able to recover the local strain at any point of the composite when the average strain $\overline{\mathbf{e}}$ is prescribed.
The average stress in the whole unit cell Ω is obtained as:

$$\begin{aligned} \overline{\boldsymbol{\sigma}}^{\overline{\mathbf{e}}} &= \frac{1}{V^{\Omega}}\left[\int_{\Omega^i} \mathbf{C}^{\Omega^i}\,\mathbf{e}\,dV + \int_{\Omega^e} \mathbf{C}^{B}\,\mathbf{e}\,dV\right] = \\ &= \frac{1}{V^{\Omega}}\left[\mathbf{C}^{\Omega^i}\,\overline{\mathbf{R}}^{\Omega^i} V^{\Omega^i} + \mathbf{C}^{B}\,\overline{\mathbf{R}}^{\Omega^e} V^{\Omega^e}\right]\overline{\mathbf{e}} = \overline{\mathbf{C}}\,\overline{\mathbf{e}} \end{aligned} \tag{18}$$

where V^{Ω} is the total volume of the UC, $\overline{\mathbf{R}}^{\Omega^i}$ and $\overline{\mathbf{R}}^{\Omega^e}$ are defined as:

$$\overline{\mathbf{R}}^{\Omega^j} = \frac{1}{V^{\Omega^j}}\int_{\Omega^i} \mathbf{R}(x_1,x_2)\,dV \qquad \overline{\mathbf{R}}^{\Omega^e} = \frac{1}{V^{\Omega^e}}\int_{\Omega^e} \mathbf{R}(x_1,x_2)\,dV \tag{19}$$

$\overline{\mathbf{C}}$ represents the overall elastic constitutive matrix, $\mathbf{C}^{\Omega^i}=\mathbf{C}^{M}$ or $\mathbf{C}^{\Omega^i}=\mathbf{C}^{B}$ when Ω^i is a sub-domain of the mortar or of the brick, respectively, and V^{Ω^j} and V^{Ω^e} are the volumes of Ω^j and Ω^e.

Inelastic strain $\boldsymbol{\pi}^i$

The inelastic strain in the typical sub-domain Ω^i is represented in the form:

$$\begin{aligned} \boldsymbol{\pi}^i &= \boldsymbol{\pi}_0^i + x_1\boldsymbol{\pi}_1^i + x_2\boldsymbol{\pi}_2^i + x_1x_2\boldsymbol{\pi}_3^i \\ &= \hat{\boldsymbol{\pi}}_0^i + \hat{\boldsymbol{\pi}}_1^i + \hat{\boldsymbol{\pi}}_2^i + \hat{\boldsymbol{\pi}}_3^i \end{aligned} \tag{20}$$

When an inelastic strain contribution $\hat{\boldsymbol{\pi}}_k^i$, with $i=1,...,n$ and $k=0,1,2,3$, is prescribed in Ω^i, under the condition of null average strain in the whole UC, the solution is determined in form:

$$\mathbf{q}_k^i\left(x_1,x_2\right)=\mathbf{Q}_k^i\left(x_1,x_2\right)\boldsymbol{\pi}_k^i \qquad \text{(no sum)} \tag{21}$$

with $\mathbf{Q}_k^i\left(x_1,x_2\right)$ representing the localization matrix associated to the presence of the inelastic strain contribution $\hat{\boldsymbol{\pi}}_k^i$ in Ω^i. It can be remarked that the field $\mathbf{q}_k^i\left(x_1,x_2\right)$ is periodic in Ω, so that its average in the UC is null, i.e. $\overline{\mathbf{q}}_k^i=0$. The elastic strains in Ω^j and Ω^e, due to $\hat{\boldsymbol{\pi}}_k^i$ in Ω^i, are obtained as:

$$\boldsymbol{\eta}_k^{i,\Omega^j}=\left(\mathbf{Q}_k^{i,\Omega^j}-\delta_{ij}\mathbf{I}_k\right)\boldsymbol{\pi}_k^i \qquad \boldsymbol{\eta}_k^{i,\Omega^e}=\mathbf{Q}_k^{i,\Omega^e}\boldsymbol{\pi}_k^i \tag{22}$$

being $\mathbf{Q}_k^{i,\Omega^j}$ and $\mathbf{Q}_k^{i,\Omega^e}$ the restrictions of the field $\mathbf{Q}_k^i$ to Ω^i and Ω^e and $\mathbf{I}_0=\mathbf{I}$, $\mathbf{I}_1=x_1\mathbf{I}$, $\mathbf{I}_2=x_2\mathbf{I}$ and $\mathbf{I}_3=x_1x_2\mathbf{I}$.
Note that $\boldsymbol{\eta}_k^{i,\Omega^j}$ is the elastic strain in the sub-domain Ω^j due to the presence of the inelastic strain contributions $\hat{\boldsymbol{\pi}}_k^i$, acting in the sub-domain Ω^i.
It can be remarked that the strain field $\mathbf{q}_k^i\left(x_1,x_2\right)$ is characterized by non zero average stress:

$$\begin{aligned}\overline{\boldsymbol{\sigma}}^{\pi_k^i}&=\frac{1}{V^\Omega}\left[\sum_{j=1}^{n}\mathbf{C}^{\Omega^j}\int_{\Omega^j}\left(\mathbf{Q}_k^{i,\Omega^j}-\delta_{ij}\mathbf{I}_k\right)dV+\mathbf{C}^B\int_{\Omega^e}\mathbf{Q}_k^{i,\Omega^e}\,dV\right]\boldsymbol{\pi}_k^i\\&=\frac{1}{V^\Omega}\left[\sum_{j=1}^{n}\mathbf{C}^{\Omega^j}\left(\overline{\mathbf{Q}}_k^{i,\Omega^j}-\delta_{ij}\overline{\mathbf{I}}_k^{\Omega^j}\right)V^{\Omega^j}+\mathbf{C}^B\overline{\mathbf{Q}}_k^{i,\Omega^e}V^{\Omega^e}\right]\boldsymbol{\pi}_k^i\\&=\mathbf{S}_k^i\boldsymbol{\pi}_k^i\end{aligned} \tag{23}$$

with $\overline{\mathbf{I}}_k^{\Omega^j}V^{\Omega^j}=\int_{\Omega^j}\mathbf{I}_k\,dV$.

Overall behavior of UC

Superposing the effects generated by the application of the average strain $\overline{\mathbf{e}}$ on the whole masonry UC and the inelastic strain contributions $\hat{\boldsymbol{\pi}}_k^i$ in each sub-domain Ω^i ($i=1,..,n$), it is possible to evaluate the overall behavior of the UC. In fact, the overall average strain acting on the UC, is obtained as:

$$\overline{\boldsymbol{\varepsilon}}=\overline{\mathbf{e}}+\overline{\mathbf{q}}=\overline{\mathbf{e}} \tag{24}$$

Analogously, the overall average stress $\overline{\boldsymbol{\sigma}}$ is obtained as the sum of the average stress associated to $\overline{\mathbf{e}}$ and to $\hat{\boldsymbol{\pi}}_k^i$:

$$\overline{\boldsymbol{\sigma}}=\overline{\boldsymbol{\sigma}}^{\overline{\mathbf{e}}}+\sum_{j=1}^{n}\sum_{k=0}^{3}\overline{\boldsymbol{\sigma}}^{\pi_k^i}=\overline{\mathbf{C}}\overline{\mathbf{e}}+\sum_{j=1}^{n}\sum_{k=0}^{3}\mathbf{S}_k^i\boldsymbol{\pi}_k^i=\overline{\mathbf{C}}\left(\overline{\boldsymbol{\varepsilon}}-\overline{\mathbf{p}}\right) \tag{25}$$

where

$$\overline{\mathbf{p}}=-\sum_{j=1}^{n}\sum_{k=0}^{3}\overline{\mathbf{C}}^{-1}\mathbf{S}_k^i\boldsymbol{\pi}_k^i \tag{26}$$

represents the overall inelastic strain.
In order to evaluate the nonlinear behavior of the typical sub-domain, according to the model described in the previous section, it is necessary to evaluate the strain and the stress in suitable number of points of each sub-domain. It can be remarked that, as the inelastic strain is bilinear and it is obtained as sum of four contributions, the required number of points is equal at least to four.
Thus, chosen a typical point $P=\left(x_1^P,x_2^P\right)$ belonging to the sub-domain Ω^j or Ω^e, the total and the elastic strains, $\boldsymbol{\varepsilon}^{\Omega^j}$ and $\boldsymbol{\eta}^{\Omega^j}$ as well as $\boldsymbol{\varepsilon}^{\Omega^e}$ and $\boldsymbol{\eta}^{\Omega^e}$, are evaluated as:

$$\boldsymbol{\varepsilon}^{\Omega^j}\left(x_1^P,x_2^P\right)=\mathbf{R}^{\Omega^j}\left(x_1^P,x_2^P\right)\overline{\mathbf{e}}+\sum_{i=1}^{n}\sum_{k=0}^{3}\mathbf{Q}_k^{i,\Omega^j}\left(x_1^P,x_2^P\right)\boldsymbol{\pi}_k^i$$
$$\boldsymbol{\eta}^{\Omega^j}\left(x_1^P,x_2^P\right)=\mathbf{R}^{\Omega^j}\left(x_1^P,x_2^P\right)\overline{\mathbf{e}}+\sum_{i=1}^{n}\sum_{k=0}^{3}\left(\mathbf{Q}_k^{i,\Omega^j}\left(x_1^P,x_2^P\right)-\delta_{ij}\mathbf{I}_k\left(x_1^P,x_2^P\right)\right)\boldsymbol{\pi}_k^i \quad (27)$$

$$\boldsymbol{\varepsilon}^{\Omega^e}\left(x_1^P,x_2^P\right)=\boldsymbol{\eta}^{\Omega^e}\left(x_1^P,x_2^P\right)=\mathbf{R}^{\Omega^e}\left(x_1^P,x_2^P\right)\overline{\mathbf{e}}+\sum_{i=1}^{n}\sum_{k=0}^{3}\mathbf{Q}_k^{i,\Omega^e}\left(x_1^P,x_2^P\right)\boldsymbol{\pi}_k^i \quad (28)$$

As a consequence, the stresses at the typical point $P=\left(x_1^P,x_2^P\right)$ of Ω^j or Ω^e result:

$$\boldsymbol{\sigma}^{\Omega^j}\left(x_1^P,x_2^P\right)=\mathbf{C}^{\Omega^j}\boldsymbol{\eta}^{\Omega^j}\left(x_1^P,x_2^P\right) \quad (29)$$

$$\boldsymbol{\sigma}^{\Omega^e}\left(x_1^P,x_2^P\right)=\mathbf{C}^{B}\boldsymbol{\eta}^{\Omega^e}\left(x_1^P,x_2^P\right) \quad (30)$$

It can be noted that in some cases the inelastic strain $\boldsymbol{\pi}^i$ in some sub-domain Ω^i ($i=1,..,n$) can be considered reasonably constant so that two types of sub-domains can be distinguished:

- a set of sub-domain $\tilde{\Omega}^i$ with $i=1,..,n^c$, where $\boldsymbol{\pi}^i$ is constant, i.e. $\boldsymbol{\pi}^i=\boldsymbol{\pi}_0^i$ and $\boldsymbol{\pi}_1^i=\boldsymbol{\pi}_2^i=\boldsymbol{\pi}_3^i=\mathbf{0}$;
- a set of sub-domain $\hat{\Omega}^i$ with $i=1,..,n^l$, where $\boldsymbol{\pi}^i$ is bilinear, given by formula (20).

In such a case, the UC is subjected to:

- the average strain $\overline{\mathbf{e}}$ on the whole masonry unit cell,
- the inelastic constant strain $\boldsymbol{\pi}^i$ in each sub-domain $\tilde{\Omega}^i$ ($i=1,..,n^c$).
- the inelastic bilinear strain $\boldsymbol{\pi}^i$ in each sub-domain $\hat{\Omega}^i$ ($i=1,..,n^l$).

In order to evaluate the overall mechanical response of the UC, the procedure described above is simplified, assuming in the sub-domain $\tilde{\Omega}^i$ with $i=1,..,n^c$, $\boldsymbol{\pi}^i=\boldsymbol{\pi}_0^i$. It can be emphasized that, in this sub-domain $\tilde{\Omega}^i$, the nonlinear behavior can be governed by the average value of the total and elastic strains, evaluated as:

$$\overline{\boldsymbol{\varepsilon}}^{\tilde{\Omega}^j}=\overline{\mathbf{R}}^{\tilde{\Omega}^j}\overline{\mathbf{e}}+\sum_{i=1}^{n^l}\sum_{k=0}^{3}\overline{\mathbf{Q}}_k^{i,\tilde{\Omega}^j}\boldsymbol{\pi}_k^i+\sum_{i=1}^{n^c}\overline{\mathbf{Q}}^{i,\tilde{\Omega}^j}\boldsymbol{\pi}^i \quad (31)$$

$$\overline{\boldsymbol{\eta}}^{\tilde{\Omega}^j}=\overline{\mathbf{R}}^{\tilde{\Omega}^j}\overline{\mathbf{e}}+\sum_{i=1}^{n^l}\sum_{k=0}^{3}\left(\overline{\mathbf{Q}}_k^{i,\tilde{\Omega}^j}-\delta_{ij}\overline{\mathbf{I}}_k^{\tilde{\Omega}^j}\right)\boldsymbol{\pi}_k^i+\sum_{i=1}^{n^c}\left(\overline{\mathbf{Q}}^{i,\tilde{\Omega}^j}-\delta_{ij}\mathbf{I}\right)\boldsymbol{\pi}^i \quad (32)$$

NUMERICAL RESULTS

Some numerical applications are carried out, in order to validate the proposed model and the developed nonlinear homogenization procedure.

Two different masonries characterized by the same type of texture but different material and geometrical data, are considered. In particular, isotropic response of the blocks and mortar is assumed. The geometry and the material properties adopted for the computations are the following:

- *masonry M1*
  - material

    for the block the elastic modulus and the Poisson ratio are set $E^B=16700\text{ MPa}$, $\nu^B=0.15$, $\varepsilon_{N,o}=0.0001$ and $\gamma_{NT,o}=0.0004$, $\sigma_{N,o}=1.67\text{MPa}$ and $\tau_{NT,o}=2{,}90\text{MPa}$, $G_{cI}=0.00144\text{ N/mm}^2$ and $G_{cII}=0.0058\text{ N/mm}^2$ and μ=0.5; for the mortar it is set $E^M=798\text{ MPa}$, $\nu^M=0.11$, $\varepsilon_{N,o}=0.0003$ and $\gamma_{NT,o}=0.001$, $\sigma_{N,o}=0.24\text{MPa}$ and $\tau_{NT,o}=0.36\text{MPa}$, $G_{cI}=0.00018\text{ N/mm}^2$ and $G_{cII}=0.00126\text{ N/mm}^2$ and μ=0.75, if not differently specified;

  - geometry

    $b = 210$ mm , $h = 52$ mm and $s = 10$ mm ;
- *masonry M2*
  - material

    for the block the elastic modulus and the Poisson ratio are set $E^B = 18000$ MPa , $\nu^B = 0.15$, $\varepsilon_{N,o} = 0.0001$ and $\gamma_{NT,o} = 0.0004$, $\sigma_{N,o} = 1.80$ MPa and $\tau_{NT,o} = 3{,}13$ MPa , $G_{cI} = 0.00125$ N/mm^2 and $G_{cII} = 0.0125$ N/mm^2 and μ=0.5 ,; for the mortar it is set $E^M = 1000$ MPa , $\nu^M = 0.15$, $\varepsilon_{N,o} = 0.0005$ and $\gamma_{NT,o} = 0.001$, $\sigma_{N,o} = 0.50$ MPa and $\tau_{NT,o} = 0.4348$ MPa , $G_{cI} = 0.00125$ N/mm^2 and $G_{cII} = 0.00217$ N/mm^2 and μ=0.5 , if not differently specified;
  - geometry

    $b = 240$ mm , $h = 120$ mm and $s = 10$ mm .

Computations are developed for walls characterized by unit thickness.
The validation of the nonlinear numerical homogenization is performed comparing the results obtained by the proposed procedure with the ones determined by micromechanical Finite Element Analyses (FEA). In particular, a 2D 4-node finite element is formulated considering the different constitutive laws for bricks, head joints and bed joints and it has been implemented in the code FEAP [14]. In particular, the damage-plastic constitutive law described in Eqs. (1) – (12) is considered for mortar joints and for the block layer aligned with the mortar head joints, while the linear elastic relationship, Eq. (13), is assumed for elastic parts of the blocks. In order to avoid strain and damage localization in the mortar joints, a nonlocal integral model is adopted, defining the nonlocal equivalent strain measures as:

$$\overline{Y}_{\bullet} = \frac{\int_{\Omega^*} Y_{\bullet}\, \psi\left(\mathbf{x}-\mathbf{y}\right) dA}{\int_{\Omega^*} \psi\left(\mathbf{x}-\mathbf{y}\right) dA} \tag{33}$$

where the subscript symbol $\bullet$ stands for $_H$, $_V$ or $_\gamma$, $\mathbf{y}$ is a typical point where nonlinear constitutive law is assumed and ψ is the standard Gaussian weight function, namely:

$$\psi = \exp\left(-\frac{\left|\mathbf{x}-\mathbf{y}\right|^2}{\rho^2} \right) \tag{34}$$

with ρ = 15 mm. The above nonlocal equivalent strain measures are then used to evaluate the strain ratios defined by formulas (10).
As concerning the proposed numerical homogenization procedure, the adoption of a regularization technique should be not required because of the assumed distribution of the inelastic strain in each mortar joint.
The nonlinear behavior of the masonry unit cell is investigated considering the two types of loading histories.

First type of loading history

The unit cell of masonry material is initially subjected to a constant compressive vertical strain and, then, to a tensile loading-unloading horizontal strain history, according to the scheme illustrated in Fig. 4 and to the following table:

	t = 0 s	t = 1 s	t = 2 s	t = 2 s
$\overline{\varepsilon}_{22}$	0.0	*p*	*p*	*p*
$\overline{\varepsilon}_{11}$	0.0	0.0	0.003	-0.0005

In particular, three different values of the compressive average strain are considered: $\overline{\varepsilon}_{22} = p = 0.0$, $\overline{\varepsilon}_{22} = p = -0.0004$ and $\overline{\varepsilon}_{22} = p = -0.0008$ in order to evaluate the influence of the compressive strain on the overall behavior of the masonry.

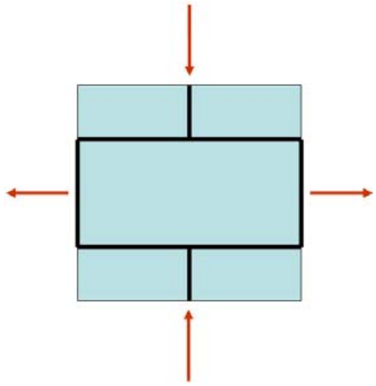

Figure 4: First type of loading history; constant vertical compression with cyclic horizontal strain.

In Figs. 5 and 6, the mechanical response of the masonry unit cell subjected to the first type of loading history characterized by the material M1 and M2 is reported, respectively. In particular, the plots of the average normal stress $\bar{\sigma}_{11}$ in the unit cell versus the total average strain $\bar{\varepsilon}_{11}$ are reported for the different values of the average compressive strains. In the Figures the results obtained by the proposed nonlinear homogenization TFA and the micromechanical analyses FEA are reported and compared.

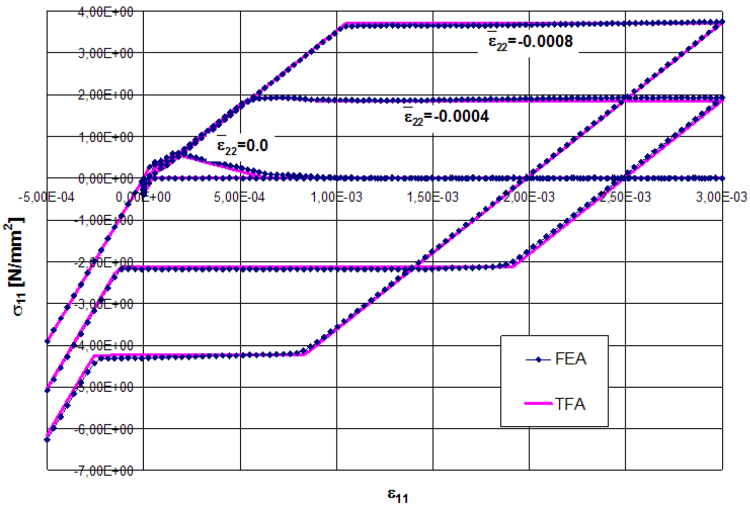

Figure 5: Mechanical response of the unit cell M1 subjected by the first loading history.

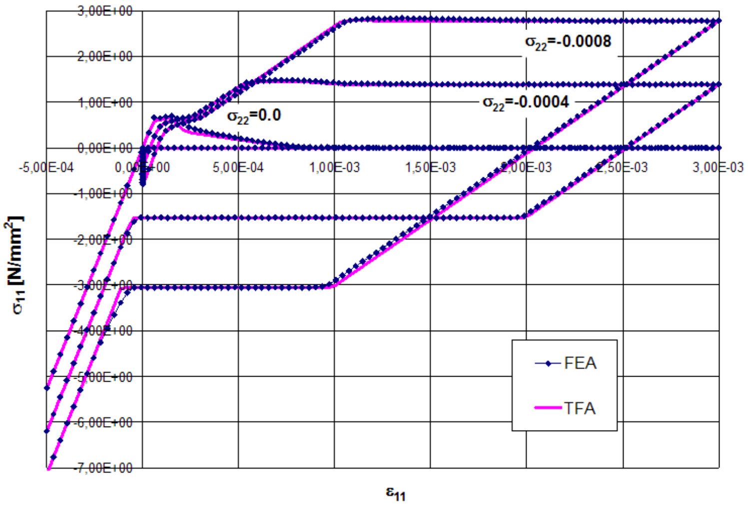

Figure 6: Mechanical response of the unit cell M2 subjected by the first loading history.

It can be noted that initially, when the unit cell is subjected to the compressive strain $\bar{\varepsilon}_{11}$, a negative average normal stress $\bar{\sigma}_{11}$ arises, because of the Poisson effect; then, the behavior of the composite material is characterized by a linear response until the vertical mortar joint starts to damage. Then, also the horizontal joints start to damage. When the mortar joints are completely damaged a friction slip occurs. The unloading path is elastic, characterized by a stiffness reduced with respect to the initial one, because of the complete damage of the mortar joints. The reverse loading is characterized by the progressive reduction of the friction slip strain; when the vertical joint is closed, the unilateral effect occurs and the initial elastic stiffness of the unit cell is recovered.
It can be pointed out that the results obtained by the nonuniform TFA and by the FEA are in very good accordance for all the three values of the average compressive strains.
In Figs. 7 and 8 the mechanical response of the masonry unit cell for $\bar{\varepsilon}_{22} = p = -0.0004$ is reported comparing the results obtained considering uniform TFA, i.e. assuming constant eigenstrains in all the 5 subsets Ω^j with *j*=1..5 or nonuniform TFA characterized by constant eigenstrains in the subsets Ω^j with *j*=1,2,3,5 and by bilinear eigenstrain in the subset Ω^4 with π^4 given by formula (20), for the material M1 and M2, respectively. It can be pointed out that for the material M2 the results obtained by the two analyses are quite in a good accordance, the uniform TFA becomes less accurate only in the unloading phase. For the material M1 characterized by a small dimension of the block, the results obtained by the uniform TFA are less accurate as in this case the nonlinear behavior of inclusion Ω^4 more significantly influences the overall response of the unit cell respect to material M2.

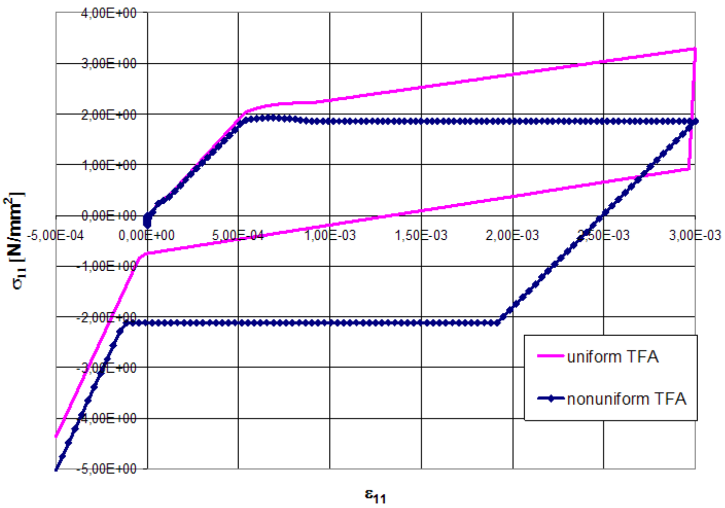

Figure 7: Mechanical response of the unit cell M1: comparison between TFA analyses.

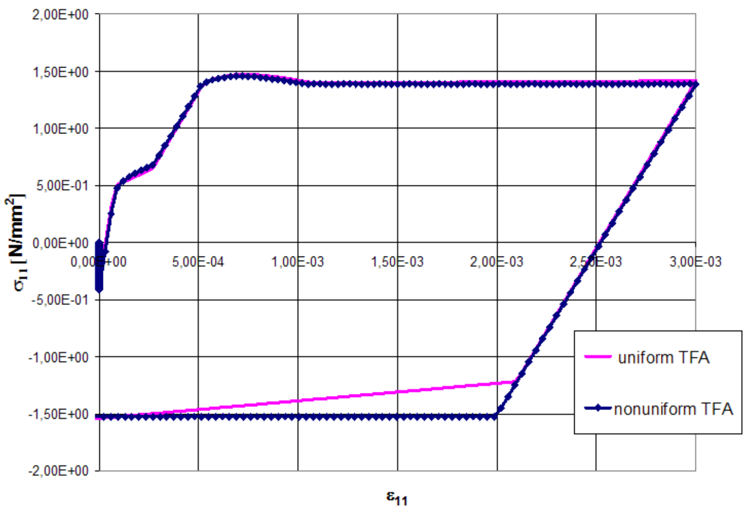

Figure 8: Mechanical response of the unit cell M2: comparison between TFA analyses.

Second type of loading history

The unit cell of masonry material is subjected to a tensile loading vertical strain history, according to the scheme illustrated in Fig. 9 and to the following table:

	t = 0 s	t = 1 s
$\bar{\varepsilon}_{22}$	0.0	0.0008

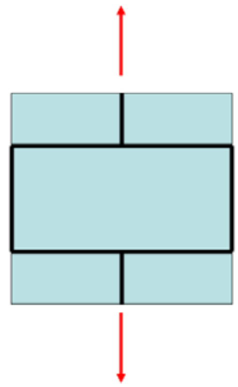

Figure 9: Second type of loading history; vertical strain.

In Fig.s 10 and 11, the mechanical response of the masonry unit cell subjected to the second type of loading history is reported for the material M1 and M2, respectively. In particular, the plot of the average normal stress $\bar{\sigma}_{22}$ in the unit cell versus the total average strain $\bar{\varepsilon}_{22}$ is given for the following three different analyses:

- uniform TFA with $\pi^i = \text{const}$ for i=1..5,
- nonuniform TFA with π^4 given by formula (20),
- FEA micromechanical analysis.

The unit cell demonstrates a pure damage mechanical response. In fact, the behavior of the masonry in vertical direction is characterized, initially, by a linear response until the horizontal mortar joints start to damage, and then, by a softening branch until the horizontal joints are completely damaged. The inelastic behavior of the unit cell is due to the damage effect, as no plastic strains occur. When the damage in the horizontal mortar joints is complete the normal stress $\bar{\sigma}_{22}$ goes to zero. It can be noted that the results obtained by the TFA analyses are in very good accordance while the FEA results slightly differs from the others only in the softening phase.

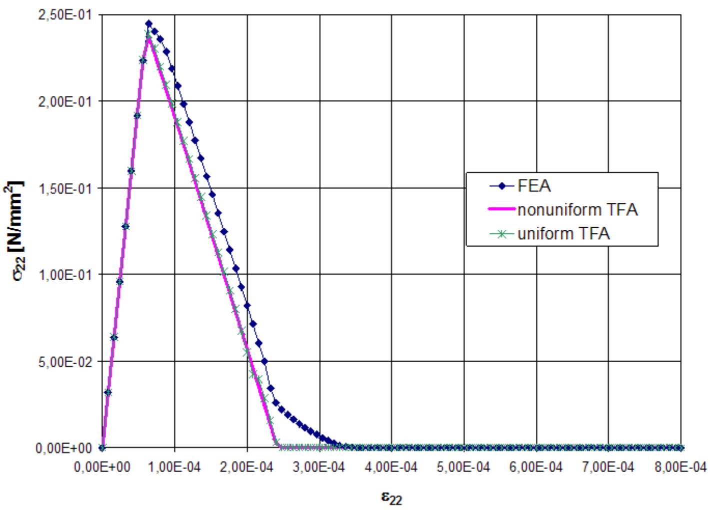

Figure 10: Mechanical response of the unit cell M1 subjected by the second loading history.

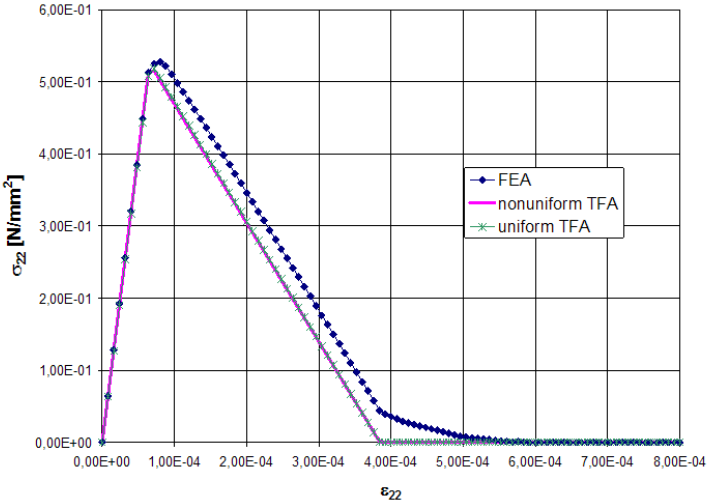

Figure 11: Mechanical response of the unit cell M2 subjected by the second loading history.

CONCLUSIONS

A nonuniform TFA technique has been proposed. The unit cell, representative of the periodic composite material, is regarded as the union of subsets, some of which present a nonlinear behavior. The nonlinearities in these subsets are accounted for by means of eigenstrain. The main and nontrivial novelty of the paper consists in assuming that the eigenstrain the each subset is not constant but it has a bilinear shape.

Numerical results, developed for different masonry UCs, show the effectiveness of the proposed technique. In fact, the uniform TFA results less accurate when the dimensions of the block are smaller so the nonlinear behavior of the head-bed mortar intersection more significantly influences the overall mechanical response of the UC. The numerical results shows that the results obtained by the nonuniform TFA are in good accordance with the once obtained by micromechanical finite element analyses.

ACKNOWLEDGMENTS

The financial supports of the Italian National Research Council (CNR), of the Consorzio RELUIS (Department of Civil Protection) are gratefully acknowledged.

REFERENCES

[1] P. M. Suquet, in Homogenization Techniques for Composite Media, (Edited by E. Sanchez-Palencia and A. Zaoui), Springer-Verlag, Lecture Notes in Physics, 272 (1987).
[2] R. Luciano, E. Sacco, Eur. J. Mech. A/Solids, 17 (1998) 599.
[3] B. Kralj, G. K. Pande, J. Middleton, Computers and Structures, 41 (1991) 53.
[4] S. Pietruszczak, X. Niu, Int. J. Solids Struct, 29 (1992) 531.
[5] L. Gambarotta, S. Lagomarsino, Earthquake Eng Struct Dynam, 26 (1997) 441.
[6] G. Uva, G. Salerno, Int. J. Solids Struct, 43 (2006) 3739.
[7] R. Luciano, E. Sacco, Int. J. Solids Struct, 34 (1997) 3191.
[8] G. Dvorak, Proc. Roy. Soc. London A, 437 (1992) 311.
[9] J. Fish, K. Shek, Composites Science and Technology, 60 (2000) 2547.
[10] J. Chaboche, L. S. Kruch, J. Maire, T. Pottier, Int. J. of Plasticity, 17 (2001) 411.
[11] J. Michel, P. Suquet, Int. J. Solids Struct., 40 (2003) 6937.
[12] E. Sacco, Eur. J. Mech. A/Solids, 28 (2009) 209.

[13] D. Addessi, E. Sacco, A. Paolone, Equivalent Cosserat Model for Periodic Masonry Deduced by a Nonlinear Homogenization TFA Procedure. Submitted for the publication on an International Journal (2009).
[14] O. C. Zienkiewicz, R. L. Taylor, The finite element method. Fourth ed. McGraw-Hill, London (1994).